PERGAMON

Chemical Engineering Science 55 (2000) 6139–6154

Chemical Engineering Science

Development of a dynamic nonequilibrium cell model for reactive distillation tray columns

R. Baur[a,b], R. Taylor[b,c], R. Krishna[a,*]

[a]*Department of Chemical Engineering, University of Amsterdam, Nieuwe Achtergracht 166, 1018 WV Amsterdam, The Netherlands*
[b]*Department of Chemical Engineering, Clarkson University, Potsdam, NY 13699-5705, USA*
[c]*Department of Chemical Technology, University of Twente, 7500 AE Enschede, The Netherlands*

Received 10 March 2000; accepted 23 June 2000

Abstract

In this paper we develop a nonequilibrium (NEQ) cell model to describe the dynamic operation of reactive distillation (RD) tray columns. The features of our model are: (1) use of the Maxwell–Stefan equations for describing mass transfer between fluid phases, (2) chemical reactions are assumed to take place only in the liquid phase, (3) coupling between mass transfer and chemical reactions within the diffusion layer is accounted for, and (4) the use of multiple well-mixed cells in the liquid and vapour flow directions accounts for staging in either fluid phase. When the chemical reactions are suppressed, our model describes the dynamic behaviour of conventional distillation columns. We demonstrate the utility of the dynamic NEQ cell model by means of three case studies: (1) metathesis of 2-propene in an RD column, (2) distillation of methanol–*iso*-propanol–water, and (3) synthesis of methyl *tert*-butyl ether (MTBE) in an RD column. For comparison purposes we have also carried out dynamic simulations using the equilibrium stage (EQ) model. These case studies help us to draw the following conclusions. The introduction of staging in the liquid and vapour phases not only influences the steady-state performance, by increasing reaction conversion and separation capability, but also has a significant influence on column dynamics. With multiple cells per stage the column dynamics becomes much more sensitive to perturbations. Furthermore, we show that even when the NEQ cell model and EQ stage model exhibit almost identical *steady-state* characteristics, the *dynamic* responses of an RD column could even be *qualitatively* different. When operating close to the distillation boundary for nonreactive, conventional, distillation, small disturbances in feed compositions can lead to completely different product compositions.

Keywords: Reactive distillation; Equilibrium stage model; Nonequilibrium cell model; Multiple steady states; Dynamics; Maxwell–Stefan equations; Methyl *tert*-butyl ether synthesis; Metathesis reaction

1. Introduction

The design and operation issues for reactive distillation (RD) systems are considerably more complex than those involved for either conventional reactors or conventional distillation columns. The introduction of an in situ separation function within the reaction zone leads to complex interactions between vapour–liquid equilibrium, vapour–liquid mass transfer, intra-catalyst diffusion (for heterogeneously catalysed processes) and chemical kinetics. Such interactions have been shown to lead the phenomenon of multiple steady states and complex dynamics. In the literature, there has also been considerable attention to the phenomena of multiple steady states. Using the equilibrium (EQ) stage model, steady-state multiplicities have been reported for applications such as synthesis of methyl *tert*-butyl ether (MTBE) (Güttinger & Morari, 1999a,b; Jacobs & Krishna, 1993; Mohl et al., 1999; Nijhuis, Kerkhof & Mak, 1993; Hauan, Hertzberg & Lien, 1995), synthesis of ETBE (Sundmacher, Uhde & Hoffmann, 1999), synthesis of TAME (Mohl et al., 1999; Rapmund, Sundmacher & Hoffmann, 1998) and for production of ethylene glycol (Ciric & Miao, 1994; Kumar & Daoutidis, 1999). More recent work (Baur, Higler, Taylor & Krishna, 2000; Higler, Taylor & Krishna, 1999c,d; Higler, Krishna & Taylor, 1999a, 2000) have used the nonequilibrium (NEQ) model to examine steady-state multiplicities in MTBE synthesis and for ethylene glycol production.

* Corresponding author. Tel.: + 31-20-525-7007; fax: + 31-20-525-5604.
E-mail address: krishna@its.chem.uva.nl (R. Krishna).

0009-2509/00/$ - see front matter
PII: S0009-2509(00)00204-9

To describe the dynamics of RD columns, three types of models exist in the literature (a comprehensive review is available in Taylor and Krishna (2000)):

(1) Equilibrium (EQ) stage model (Abufares & Douglas, 1995; Bartlett & Wahnschafft, 1998; Espinosa, Martinez & Perez, 1994; Grosser, Doherty & Malone, 1987; Kumar & Daoutidis, 1999; Moe, Hauan, Lien & Hertzberg, 1995; Perez-Cisneros, Schenk, Gani & Pilavachi, 1996; Scenna, Ruiz & Benz, 1998; Schrans, de Wolf & Baur, 1996; Sneesby, Tadé & Smith, 1998),
(2) EQ stage model with fixed stage efficiencies (Alejski & Duprat, 1996; Ruiz, Basualdo & Scenna, 1995), and
(3) Nonequilibrium (NEQ) stage model for packed RD column (Kreul, Gorak, Dittrich & Barton, 1998).

Roat, Downs, Vogel and Doss (1986) integrate the control system equations with the EQ stage model equations and show, using the Eastman methyl acetate process, that control schemes with good steady-state characteristics may fail under unsteady-state conditions. Besides the methyl acetate process, there are other RD processes such as the synthesis of ethylene glycol that are carried out in tray columns in which the contacting pattern on any stage is cross-current. For large diameter columns used in industry there will be sufficient staging in both the vapour and liquid phases. In a recent paper Muller and Segura (2000) have demonstrated the importance of cross-flow effects and staging on the separation performance of conventional (nonreactive) distillation.

Liquid-phase staging is considerably more important for RD operations than for conventional distillation because of its influence on conversion and selectivity. The assumption of well-mixed vapour and liquid phases, made in all published EQ and NEQ models, does not hold for such RD tray columns. The primary objective of our paper is to develop a rigorous dynamic NEQ model for RD columns, which would cater for cross-flow contacting of vapour and liquid phases by dividing the stage into a number of well-mixed cells in the liquid and vapour flow directions.

When the chemical reactions are suppressed, our model describes the dynamics of conventional multicomponent distillation tray column and extends the earlier work of Kooijman and Taylor (1995).

We underline the various features of the developed dynamic NEQ cell model by means of three case studies: (1) metathesis of 2-propene in an RD column, (2) distillation of methanol–isopropanol–water, and (3) synthesis of MTBE in an RD column.

2. Dynamic nonequilibrium (NEQ) cell model development

The basic idea of the NEQ cell model is shown in Fig. 1. Each stage is divided into a number of *contacting cells*; these cells describe just a small section of a single tray. The vapour entering a stage is divided into cells m in total, in the first horizontal row. The liquid entering the stage is, similarly, divided into cells n in total, in the first vertical column. In all of our calculations the liquid flow is divided equally into cells in a vertical column. Any feed entering the stage is also apportioned to the entering row, or column, of cells in the same manner. By choosing an appropriate number of cells in each flow direction, one can model the actual flow patterns on a tray. A column of cells can model plug flow in the vapour phase, and multiple columns of cells can model plug flow in the liquid phase. When the number of well-mixed cells in any flow direction is four or more, we have essentially plug flow of that phase. Various degrees of backmixing in the vapour and liquid phases can be modelled by choosing the number of well-mixed cells to lie between 1 and 4. Correlations are available in the literature to estimate the number of well-mixed cells in the liquid flow direction (Bennett & Grimm, 1991). The staging in the liquid phase is strongly dependent on the column diameter. Liquid-phase staging is in particular important for large-diameter columns. The assumption of plug flow for the vapour phase is a good approximation and therefore a choice of 4 cells in the vertical direction is able to deal with this situation. Further details of the implementation of the cell model can be found in Higler, Taylor and Krishna (1998) Higler et al. (1999a,c,d, 2000) and Higler, Krishna and Taylor (1999b) who have developed a steady-state version for RD columns. We first analyse the balance relations for a typical cell on a tray (cf. Fig. 1(b)).

2.1. Balance relations for cells

The dynamics of a well-mixed cell are determined, inter alia, by the storage capacity, or accumulation, of mass and energy in the vapour and liquid phases. The time rate of change of the number of moles of component i in the vapour (M_i^V) and liquid (M_i^L), are given by

$$\frac{\mathrm{d}M_i^V}{\mathrm{d}t} = V_{\mathrm{in}} y_{i,\mathrm{in}} - V y_i - \mathbb{N}_i^V, \tag{1}$$

$$\frac{\mathrm{d}M_i^L}{\mathrm{d}t} = L_{\mathrm{in}} x_{i,\mathrm{in}} - L x_i + \mathbb{N}_i^L \sum_{k=1}^{r} \nu_{i,k} R_k \varepsilon^L + L_M (x_{i,M+} + x_{i,M-} - 2x_i). \tag{2}$$

Allowance is made for a total of r (homogeneous) chemical reactions in the liquid phase with a reaction rate R_k. ε^L represents the volumetric liquid hold-up in the cell. Heterogeneous chemical reactions taking place inside catalyst particles are modelled with a pseudo-homogeneous description and use of catalyst effectiveness factors and effective reaction rate constants. The last term in

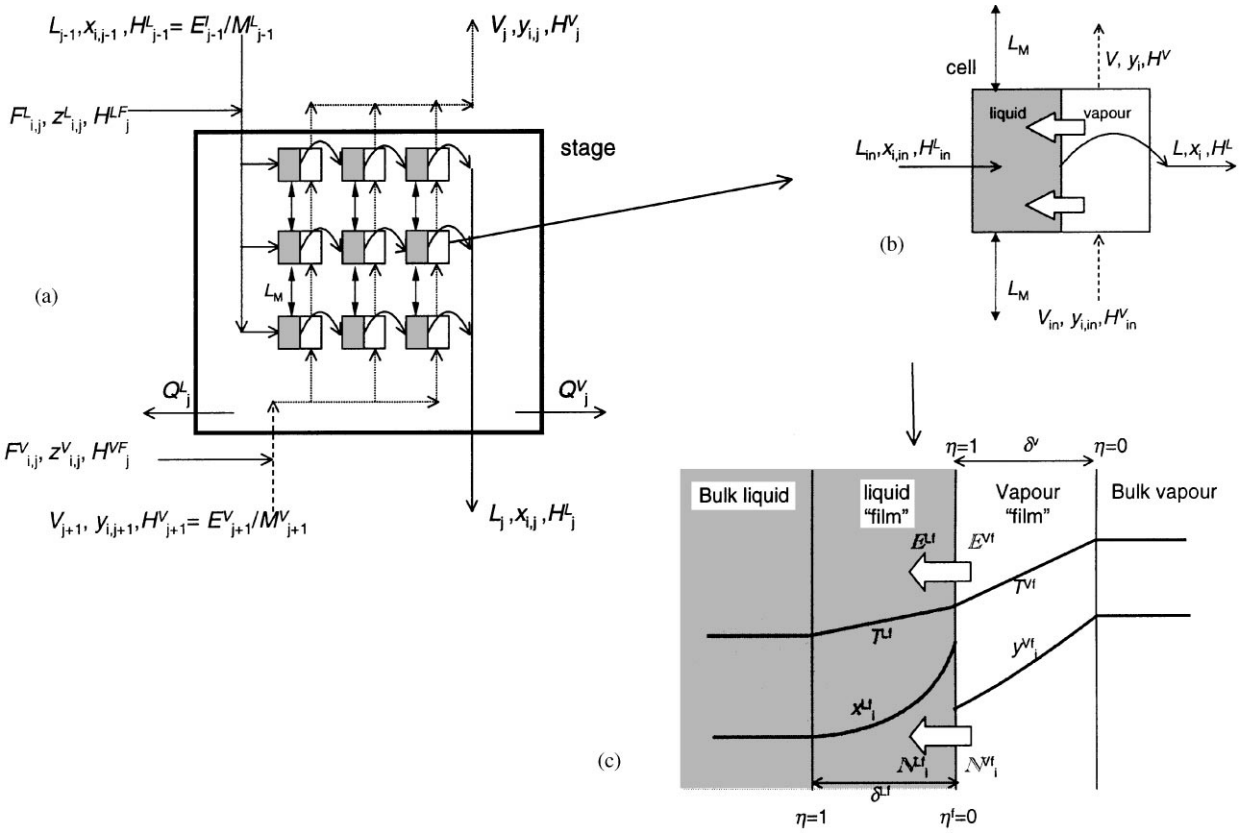

Fig. 1. (a) Schematic representation of an NEQ cell model for a stage j. (b) Balance relations for a representative cell. (c) Composition and temperature profiles within the vapour and liquid "films".

Eq. (2) describes the interchange of liquid between horizontal rows of cells, where L_M is a specified interchange liquid molar flow rate, $x_{i,M+}$ the composition in the cell above and $x_{i,M-}$ the composition in the cell below the one under consideration. In setting up the proper component and enthalpy balances for the multi-cell model we need to take the following considerations into account.

- The amount of liquid entering a cell from the cell above (below) is exactly the same as the amount of liquid leaving the cell to the cell below (above).
- The liquid mixing flow L_M is large as compared to the flow of the liquid entering and leaving each cell.

In practice the vapour jet issuing from the holes on a tray will create a "fountain" effect; this will tend to mix the liquid phase more or less completely in the vertical direction (Lockett, 1986). In order to model this situation in which the liquid compositions in any vertical column of cells have the same composition, we choose a value of L_M which is considerably larger, say 10 times, than the liquid flow on that stage. In all the calculations presented in this paper, the liquid phase in a vertical column of cells is assumed to be well mixed.

The overall molar balance for the cell is obtained by summing Eqs. (1) and (2) over the total number of components, c in the mixture

$$\frac{\mathrm{d}M^V}{\mathrm{d}t} = V_{\mathrm{in}} - V - \sum_{k=1}^{c} \mathbb{N}_k^V, \tag{3}$$

$$\frac{\mathrm{d}M^L}{\mathrm{d}t} = L_{\mathrm{in}} - L + \sum_{k=1}^{c} \mathbb{N}_i^L + \sum_{i=1}^{c}\sum_{k=1}^{r} \nu_{i,k} R_k \varepsilon^L. \tag{4}$$

The mole fractions of the vapour and liquid phases are calculated from the respective phase molar hold-ups

$$y_i = M_i^V/M^V, \qquad x_i = M_i^L/M^L. \tag{5}$$

Only $c-1$ of these mole fractions are independent because the phase mole fractions sum to unity

$$\sum_{k=1}^{c} y_k = 1, \qquad \sum_{k=1}^{c} x_k = 1. \tag{6}$$

In our model $c-1$ molar component balances (1) and (2) have been implemented along with Eqs. (3)–(6).

The phase energy balance is written in terms of the energy "hold-ups" in the cell

$$\frac{\mathrm{d}E^V}{\mathrm{d}t} = V_{\mathrm{in}}\frac{E_{\mathrm{in}}^V}{M_{\mathrm{in}}^V} - V\frac{E^V}{M^V} - \mathbb{E}^V - Q^V, \tag{7}$$

$$\frac{dE^L}{dt} = L_{in}\frac{E^L_{in}}{M^L_{in}} - L\frac{E^L}{M^L} + \mathbb{E}^L - Q^L + L_M\left(\frac{E^L_{M+}}{M^L_{M+}} + \frac{E^L_{M-}}{M^L_{M-}} - 2\frac{E^L}{M^L}\right). \quad (8)$$

The last term in Eq. (8) takes mixing perpendicular to the flow direction into account as described for the component mass balance; see Eq. (2). The heat removal from the liquid phase in each cell is simply the heat removal from stage divided by the total number of cells

$$Q^L = Q^L_j/mn, \qquad Q^V = Q^V_j/mn. \quad (9)$$

The energy hold-ups are related to the corresponding molar hold-ups via the stage enthalpies

$$E^V = H^V M^V, \qquad E^L = H^L M^L. \quad (10)$$

There is no need to take separate account in Eqs. (7) and (8) of the heat generated due to chemical reaction since the computed enthalpies include the heats of formation.

2.2. Interfacial mass and energy transfers

The resistance to mass and energy transfer is located in thin "films" adjacent to the vapour–liquid interface; see Fig. 1(c). The liquid-phase diffusion film thickness δ^{Lf} is of the order of 10 μm and the vapour-phase diffusion film thickness δ^{Vf} is of the order of 100 μm. The storage capacity for mass and energy in these films is negligibly small compared to that in the bulk fluid phases and so the interfacial transfer rates can be calculated from quasi-stationary interfacial transfer relations. The molar component balances within the film are given by

$$\frac{\partial \mathbb{N}^{Vf}_i(\eta^{Vf})}{\partial \eta^{Vf}} = 0, \quad (11)$$

$$\frac{\partial \mathbb{N}^{Lf}_i(\eta^{Lf})}{\partial \eta^{Lf}} + \sum_{k=1}^{r} \nu_{i,k} R_k(\eta^{Lf}) A\delta^{Lf} = 0. \quad (12)$$

In Eqs. (11) and (12), A represents the interfacial area and $A\delta^{Lf}$ represents the volume available for liquid-phase chemical reaction. The coupling of diffusion and chemical reaction within the liquid film is particularly important for fast chemical reactions (Hatta number exceeding unity). The molar transfer rate $\mathbb{N}_k$ is related to the chemical potential gradients by the Maxwell–Stefan equations (Krishna & Wesselingh, 1997; Taylor & Krishna, 1993, 2000)

$$\frac{y^{Vf}_i}{\mathbb{R}T^{Vf}}\frac{\partial \mu^{Vf}_i}{\partial \eta} = \sum_{k=1}^{c} \frac{y^{Vf}_i \mathbb{N}^{Vf}_k - y^{Vf}_k \mathbb{N}^{Vf}_i}{c^{Vf}_t \kappa^{Vf}_{i,k} A}, \quad (13)$$

$$\frac{x^{Lf}_i}{\mathbb{R}T^{Lf}}\frac{\partial \mu^{Lf}_i}{\partial \eta} = \sum_{k=1}^{c} \frac{x^{Lf}_i \mathbb{N}^{Lf}_k - x^{Lf}_k \mathbb{N}^{Lf}_i}{c^{Lf}_t \kappa^{Lf}_{i,k} A}. \quad (14)$$

The $\kappa_{i,k}$ represents the mass transfer coefficient of the i–k pair in the phase; this coefficient is estimated from information on the corresponding Maxwell–Stefan diffusivity $Đ_{i,k}$ using the standard procedures discussed in Taylor and Krishna (1993). Only $c-1$ of Eq. (13) or Eq. (14) are independent. The following summation equations hold:

$$\sum_{k=1}^{c} y^{Vf}_{i,j} = 1, \qquad \sum_{k=1}^{c} x^{Lf}_{i,j} = 1. \quad (15)$$

The energy balances within the diffusion film are given by

$$\frac{\partial \mathbb{E}^{Vf}}{\partial \eta^{Vf}} = 0, \qquad \frac{\partial \mathbb{E}^{Lf}}{\partial \eta^{Lf}} = 0, \quad (16)$$

where the interfacial energy transfer rate $\mathbb{E}$ has both conductive and convective contributions

$$\mathbb{E}^{Vf} = -h^{Vf}A\frac{\partial T^{Vf}}{\partial \eta} + \sum_{i=1}^{c} \mathbb{N}^{Vf}_i H_i{}^{Vf}, \ \mathbb{E}^{Lf} = -h^{Lf}A\frac{\partial T^{Lf}}{\partial \eta} + \sum_{i=1}^{c} \mathbb{N}^{Lf}_i H^{Lf}_i. \quad (17)$$

At the vapour–liquid interface we assume phase equilibrium and the mole fractions in the vapour and liquid phases are related by

$$y_i|_I = K_i x_i|_I, \qquad T^{Vf}|_I = T^{Lf}|_I. \quad (18)$$

Furthermore, the fluxes of mass and energy are continuous across the interface

$$\mathbb{N}^{Vf}_i|_I = \mathbb{N}^{Lf}_i|_I, \qquad \mathbb{E}^{Vf}|_I = \mathbb{E}^{Lf}|_I. \quad (19)$$

2.3. Link between cell variables and stage variables

The foregoing analysis pertains to each cell within the distillation tray "froth" region. We need to develop the inter-relation between the cell variables and the stage variables. The sum of the molar vapour flows leaving the top row of cells gives the total molar vapour flow leaving the stage j. A corresponding equation for last column of cells gives the total molar liquid flow leaving the stage j:

$$\sum_{mm=1}^{m} V_{mm,n} = V_j, \qquad \sum_{nn=1}^{n} L_{m,nn} = L_j. \quad (20)$$

The relations for the component molar flows are

$$\sum_{mm=1}^{m} y_{i,mm,n} V_{mm,n} = y_{i,j} V_j, \qquad \sum_{nn=1}^{n} x_{i,m,nn} L_{m,nn} = x_{i,j} L_j. \quad (21)$$

For the energy hold-ups we have

$$\sum_{mm=1}^{m} \frac{E^V_{mm,n}}{M^V_{mm,n}} V_{mm,n} = H^V_j V_j, \qquad \sum_{nn=1}^{n} \frac{E^L_{m,nn}}{M^L_{m,nn}} L_{m,nn} = H^L_j L_j. \quad (22)$$

The volumetric hold-ups per cell are — here — assumed to be a simple fraction $1/mn$ of the corresponding stage hold-ups

$$\varepsilon^V \equiv \frac{1}{c^V_{t,j}} M^V_j = \frac{1}{mn}\varepsilon^V_j, \qquad \varepsilon^L \equiv \frac{1}{c^L_{t,j}} M^L_j = \frac{1}{mn}\varepsilon^L_j. \tag{23}$$

A similar relation holds for the interfacial area:

$$A = \frac{1}{mn} A_j. \tag{24}$$

Phase equilibrium and reaction rates are calculated per cell based on the local compositions and temperature prevailing. Hydrodynamics and mass transfer parameters are calculated using stage flows, compositions and temperatures. For example, for sieve tray columns the volumetric liquid hold-up on the stage can be calculated by knowing the active (or bubbling) tray area, A_{bub}, and estimation of the clear liquid height, h_{cl} (Bennett, Agrawal & Cook, 1983; Barker & Self, 1962)

$$\varepsilon^L_j = h_{\mathrm{cl},j} A_{\mathrm{bub},j}. \tag{25}$$

From the chosen tray spacing, h_t, the corresponding volumetric vapour hold-up can be calculated

$$\varepsilon^V_j = (h_t - h_{\mathrm{cl},j}) A_{\mathrm{bub},j}. \tag{26}$$

The liquid and vapour residence times on the stage can be calculated from knowledge of the volumetric hold-ups and flows on the stage. The liquid and vapour residence times for a particular cell are calculated as follows:

$$\tau^V_{mm,nn} = \frac{1}{n}\tau^V_j, \qquad \tau^L_{mm,nn} = \frac{1}{m}\tau^L_j. \tag{27}$$

Although not done here, the hold-up in the vapour disengagement space between trays can be modelled by rows of cells containing only vapour. It would also be straightforward to use columns of liquid to model the hold-up in the downcomer of a tray column. The mass and energy transfer rate equations would not be needed for such cells.

2.4. Condenser and reboiler modelling

The liquid hold-up in the reboiler and condenser is usually much larger than the hold-up on a particular stage. High liquid hold-ups lead to operational robustness, but also cause the equations to be very stiff. In our model implementation, liquid buffers are incorporated at the top and bottom. The condenser is followed by a reflux drum buffering the condensate. A partial condenser is modelled as an equilibrium stage. The reflux drum is considered to be a well mixed system with a specified volumetric capacity. The mean liquid residence time and dynamic characteristics are therefore fully determined with this specification. The liquid leaving the bottom of the column is led to a reboiler drum with a specified volumetric capacity (hold-up) and assumed to be well mixed. The contents are then transferred to a partial, or total reboiler. A partial reboiler is modelled as an equilibrium stage.

2.5. Model system

As described above the model combines differential equations for the bulk dynamics, with partial differential equations for the transport through the film and algebraic equations for the vapour–liquid equilibrium at the interface. For the purposes of solving the transfer rate equations we divide the film into a number of slices (five in the calculations described below). The Maxwell–Stefan and energy transfer rate equations are written for each node with the derivative terms replaced by finite difference approximations. Central difference approximations should be avoided as they tend to lead to zigzag concentration profiles.

The resulting model is a set of differential-algebraic (DAE) equations and is summarised in Table 1, which also lists the variables computed by solving the model equations. The index of this DAE system is 1; the index being the minimum number of differentiations needed to obtain a system consisting only of ODEs (Unger, Kröner & Marquardt 1995; Mattsson & Sönderlind, 1993). It is useful to know the index of a DAE system because some numerical integration methods cannot reliably solve systems with an index higher than one. A higher index was avoided by making the hydrodynamics depend explicitly on the flows leaving a stage or cell, Eqs. (25)–(27), by using steady-state mass and energy transfer rate equations, and by assuming the liquid residence time to be the same in each cell. An even distribution of molar hold-ups leads to an index greater than 1.

The DAE system is solved using BESIRK (Kooijman, 1995; Kooijman & Taylor, 1995). BESIRK is a semi-implicit Runge–Kutta method originally developed by Michelsen (1976) and extended with an extrapolation scheme (Bulirsch & Stoer, 1966), improving the efficiency in solving the DAE problem. The evaluation of the sparse Jacobian required by this method is carried out primarily using analytical expressions. The exceptions include entries including derivatives of enthalpies, mass and heat transfer coefficients, hold-ups and pressure drop.

The initial condition is a solution to the steady-state equations where all time derivatives are set to zero. Following the initialisation as described, the time-dependent equations are integrated for some predetermined time. The program stops the integration after a time-dependent discontinuity is reached and re-initialises the DAE system depending on the perturbation under consideration. Perturbations in the reboiler or condenser specifications, such as reboil ratio or reflux ratio, require a consistent re-initialisation of the flows in order to satisfy the algebraic constraints. In some cases it might

Table 1
Model equations for dynamic nonequilibrium cell model . The model equations are either ordinary differential equations (ODE), partial differential equations (PDE), or algebraic equations (AE). The number of discrete points in the liquid film is denoted with nL, and in the vapour film with nV, respectively

Description of equation	Bulk liquid phase				Bulk vapour phase			
	Number of eqns	Type	Eq. no.	Variable	Number of eqns	Type	Eq. no.	Variable
Total molar balance	1	ODE	Eq. (4)	M^L	1	ODE	Eq. (3)	M^V
Molar component balance	$c-1$	ODE	Eq. (2)	M_i^L	$c-1$	ODE	Eq. (1)	M_i^V
Mole fractions	c	AE	Eq. (5)	x_i	c	AE	Eq. (5)	y_i
Summation	1	AE	Eq. (6)		1	AE	Eq. (6)	
Energy balance	1	ODE	Eq. (8)	E^L	1	ODE	Eq. (7)	E^V
Energy hold-up	1	AE	Eq. (10)	T^L	1	AE	Eq. (10)	T^V
Residence time	1	AE	Eq. (27)	L	1	AE	Eq. (27)	V
	"Film" liquid phase				"Film" vapour phase			
Molar component balance	nLc	PDE	Eq. (12)	$\mathbb{N}_i^{Lf}$	nVc	PDE	Eq. (11)	$\mathbb{N}_i^{Vf}$
Maxwell–Stefan equations	nL$(c-1)$	PDE	Eq. (14)	x_i^{Lf}	nV$(c-1)$	PDE	Eq. (13)	y_i^{Vf}
Summation	nL$\times 1$	AE	Eq. (15)		nV$\times 1$	AE	Eq. (15)	
Energy balance	nL$\times 1$	PDE	Eq. (16)	$\mathbb{E}^{Lf}$	nV$\times 1$	PDE	Eq. (16)	$\mathbb{E}^{Vf}$
Energy transfer rate	nL$\times 1$	PDE	Eq. (17)	T^{Lf}	nV$\times 1$	PDE	Eq. (17)	T^{Vf}
Total: $4c+8+\mathrm{nL}(2c+2)+\mathrm{nV}(c+2)$ implemented equations per cell								
	Stage variables liquid phase				Stage variables vapour phase			
Flow leaving the stage	1	AE	Eq. (20)	L_j	1	AE	Eq. (20)	V_j
Component molar flow	c	AE	Eq. (21)	x_{ij}	c	AE	Eq. (21)	y_{ij}
Enthalpy flow	1	AE	Eq. (22)	T_j^L	1	AE	Eq. (22)	T_j^V
Total: $(nm)(4c+8+\mathrm{nL}(2c+2)+\mathrm{nV}(c+2))+2c+4$ implemented equations per stage								

also be required to define a continuous perturbation in order to maintain consistency and continuity of the solution (Kröner, Marquardt & Gilles, 1997). This is not necessary for the feed perturbation under consideration in this paper. Our model also supports steady-state computations using Newton's method, as outlined in Taylor, Kooijman and Hung (1994). In addition, the program is equipped with a continuation method for analysis of multiple-steady-state behaviour. For more details about this continuation method the reader is referred to Wayburn and Seader (1987) and Kubicek (1976).

The simulations have been performed on a PC (Pentium II 286 MHz). A nonequilibrium model with 17 stages and 1 cell per stage contains approximately 2000 equations and requires about 30 min computing time to reach a new steady state following a perturbation. An equilibrium-stage model has about 300 equations, and needs only a couple of minutes for the same problem. The computational time increases significantly with increasing numbers of cells. A 3×3 NEQ cell model with 17 trays contains about 16,000 equations and requires about 8 h to compute the desired transience.

Interested readers can download the technical manual from our website: http://www.clarkson.edu/~chengweb/faculty/taylor/chemsep/chemsep.html, which contains details of all thermodynamics, hydrodynamics and mass transfer models for tray columns which have been implemented into our reactive distillation software. The code for these models represents a large fraction of the overall program size.

3. Case study 1: dynamics of metathesis RD column

Consider the reversible metathesis reaction of 2-pentene to 2-butene and 3-hexene:

$$\text{2-pentene} \rightleftharpoons \text{2-butene} + \text{3-hexene}. \tag{28}$$

The overall rate of reaction of 2-pentene is given by

$$R = 0.5 c_{c5} k_f (x_{c5}^2 - x_{c4} x_{c6}/K_{\mathrm{eq}}). \tag{29}$$

The forward reaction rate constant is

$$k_f = 78.2 \exp\left(-\frac{27600}{RT}\right) \quad (\mathrm{s}^{-1}) \tag{30}$$

and the equilibrium reaction rate constant

$$K_{\mathrm{eq}} = 0.25. \tag{31}$$

The metathesis reaction is most effectively carried out in an RD column in order to achieve highest possible conversions of 2-pentene (Higler et al., 1999a; Okasinski & Doherty, 1998). The RD column configuration chosen for study is essentially the same as that of Higler et al. (1999a) and consists of a 25-stage column with liquid feed of pure 2-pentene on stage 13; see Fig. 2. The feed flow rate is 10 mol/s. The condenser and top column pressures are fixed at 101.3 kPa. The RD column is constructed of sieve plates and the configuration details are given in Table 2. The pressure drop on each tray is calculated using the Bennett, Agarwal and Cook (1983) correlation. The top product flow rate is fixed at 5 mol/s. The boilup ratio is fixed at 8. For calculation of the thermodynamic properties the Peng–Robinson equation of state was used. The *A.I.Ch.E.* calculation method was used for estimation of the mass transfer coefficients in the vapour and liquid phases (for details of this model see Lockett, 1986).

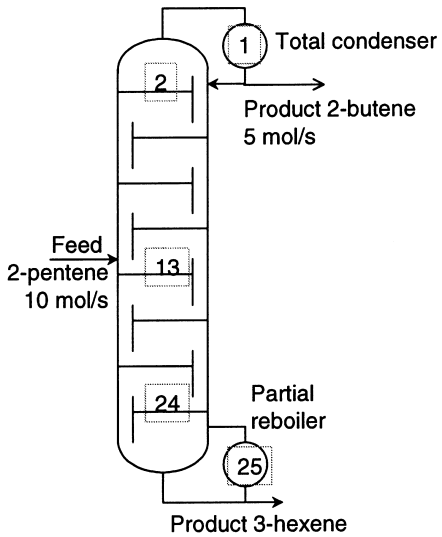

Fig. 2. Configuration of the 2-propene metathesis RD column.

Two different NEQ model implementations were used to determine the column dynamics: the NEQ 1×1 cell and NEQ 3×3 cell models. The column was operated at the initial state for a period of 1 h and the 2-pentene flow to the column was perturbed by ± 10 and $\pm 15\%$ for a period of 1 h. Fig. 3 shows the influence of staging on the dynamic response of the 2-pentene mole fraction in the top and bottom products. Firstly, we note that the composition of unreacted 2-propene in the top and bottom products at steady state is significantly lower for the NEQ 3×3 cell model. This underlines the importance of vapour- and liquid-phase staging on conversion in RD columns. Secondly, we note that the amplitude of the over(under)shoot in the 2-pentene mole fraction of the NEQ 3×3 cell model is almost as high as that of the NEQ 1×1 cell model, despite the base (steady-state) value being significantly lower. This means that the introduction of staging increases the sensitivity of the column to perturbations. This would need to be taken into account when designing controller strategies.

We also ran dynamic simulations using the EQ model. When the component efficiencies are chosen to be 0.55 for all components, the steady-state composition profiles as well as the dynamic response to perturbations obtained with the EQ model are practically indistinguishable from the results obtained with the NEQ 1×1 cell model. When the component efficiencies are chosen to be 0.74 for all components, the steady-state composition profiles as well as the dynamic response to perturbations obtained with the EQ model are practically indistinguishable from the results obtained with the NEQ 3×3 cell model. On the basis of these results one would be

Table 2
Specification of sieve tray columns used in case studies

	Case study 1: metathesis	Case study 2: MeOH–IPA–water	Case study 3: MTBE
Type of tray	Sieve	Sieve	Sieve
Column diameter (m)	1.8	0.8	6
Total tray area (m^2)	2.545	0.503	28.27
Number of liquid flow passes	2	1	5
Tray spacing (m)	0.61	0.61	0.7
Liquid flow path length (m)	0.62	0.52	0.97
Active area/total tray area	0.76	0.76	0.76
Hole diameter (m)	0.0045	0.005	0.0045
Total hole area/total tray area	0.1	0.11	0.1
Downcomer area/total tray area	0.12	0.12	0.12
Weir length (m)	3.1	0.74	22
Weir height (m)	0.08	0.05	0.05
Downcomer clearance (m)	0.038	0.038	0.038
Reboiler hold-up (m^2)	0.07	0.04	2.3
Reflux drum hold-up (m^2)	0.07	None	1.3

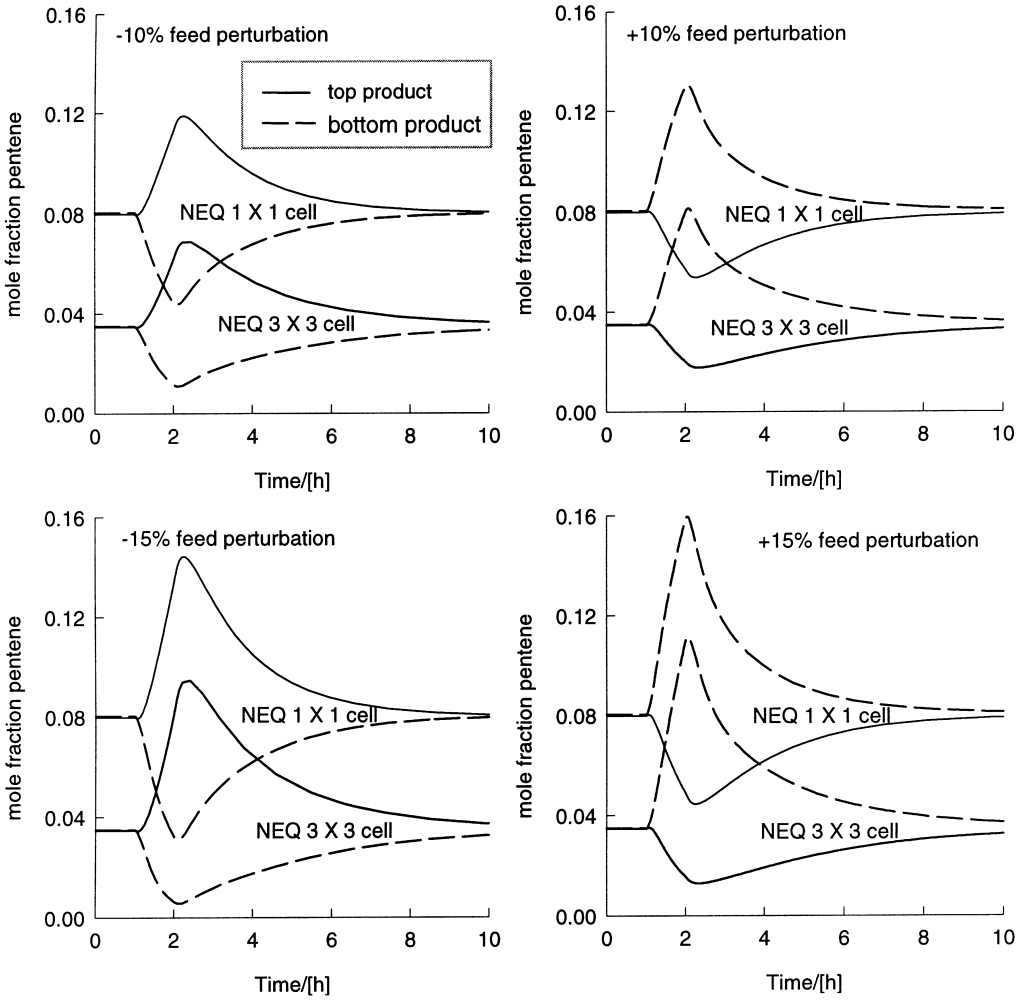

Fig. 3. Dynamic response of metathesis RD column to feed perturbations. Comparison of the response of NEQ 1×1 and NEQ 3×3 models.

tempted to conclude that the EQ model, incorporating component efficiencies, is adequate for describing RD column dynamics. We will show below in the third example on MTBE synthesis, that this conclusion is not justified in general.

4. Case study 2: dynamics of distillation of methanol–isopropanol–water

We now examine the dynamics of a conventional distillation column separating the mixture: methanol (1) –*iso*-propanol (2) –water (3). Shown in Fig. 4 are the residue curve maps (described for example in Seader & Henley, 1998) for this system, calculated using the NRTL model (with parameters listed in Table 3). The mixture has a binary minimum boiling azeotrope for *iso*-propanol–water. The distillation boundary splits the residue curve map into two regions. It can be seen that the residue curves, which originate along the distillation boundary, can choose two different paths ending up in different corners of the composition triangle. The residue curves coincide with the liquid composition trajectories during distillation at total reflux in a continuous contact device, such as a packed column, in which the liquid and vapour phases are in thermodynamic equilibrium (Baur, Taylor, Krishna & Copati, 1999).

Dynamic column simulations were carried out for a 13-stage sieve tray column, shown in Fig. 5, with the hardware specifications given in Table 2. The feed composition was chosen to lie in the distillation boundary: $x_1 = 0.5$, $x_2 = 0.35$, $x_3 = 0.15$. After steady operations for 1 h, the feed composition was perturbed to $x_1 = 0.5$, $x_2 = 0.38$, $x_3 = 0.12$. The initial and perturbed feed compositions are indicated in Fig. 4. Two types of perturbations were examined: (a) a pulsed perturbation lasting 1 h, and (b) a step perturbation. Both types of perturbations were initiated after 1 h of steady operation. The dynamic responses were calculated with three model implementations: (a) EQ model, (b) NEQ 1×1 cell model, and (c) NEQ 3×3 cell model. In the NEQ implementation the *A.I.Ch.E.* method was used for estimation

of the mass transfer coefficients in the vapour and liquid phases.

The EQ and NEQ models even predict different initial steady states! The initial steady-state column composition profiles are shown in Fig. 6. The EQ model predicts that the reboiler would consist of pure *iso*-propanol. The NEQ 3×3 cell model, on the other hand, predicts a reboiler composition which is rich in water. The NEQ 1×1 cell model, as expected, has the poorest separation capability, but the composition trajectory follows the trend of the NEQ 3×3 cell model. Introducing more stages would make the NEQ 1×1 cell model approach the separation performance of the NEQ 3×3 cell model.

Experimental data reported by Pelkonen, Kaesemann and Gorak (1997), for total reflux operation of methanol–*iso*-propanol–water in a 0.1 m diameter column packed with Sulzer BX packing, start at a composition $x_1 = 0.5$, $x_2 = 0.35$, $x_3 = 0.15$ at the top of the column and end up with virtually pure water in the reboiler. These experiments appear to verify the validity of the NEQ composition trajectories shown in Fig. 6.

The time-evolutions of the column composition profiles responding to a step feed composition perturbation are shown in Fig. 7 for the three model implementations. The incorporation of mass transfer resistance and staging increases the sensitivity of the column response. For the NEQ 3×3 cell model the reboiler composition changes from water-rich state to *iso*-propanol-rich state even for the small feed composition perturbation.

Fig. 8 compares the tray-12 composition of *iso*-propanol for both step and pulse feed composition perturbations. Again, it is clear that the NEQ 3×3 cell model is the most sensitive one. It exhibits the highest amplitude

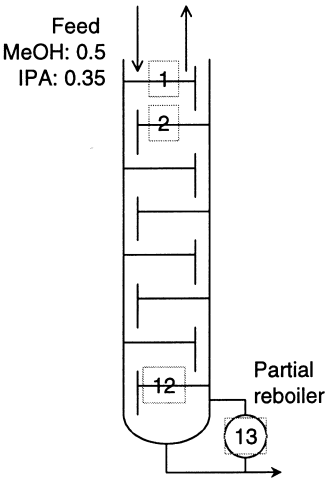

Fig. 5. Configuration of sieve tray column for separating methanol–*iso*-propanol–water.

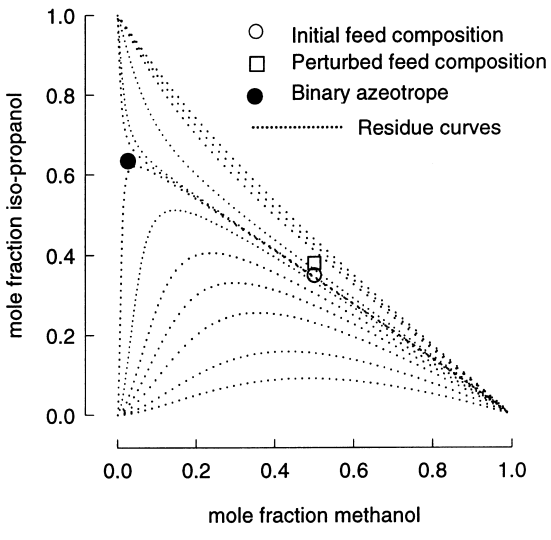

Fig. 4. Residue curve map for methanol–*iso*-propanol–water.

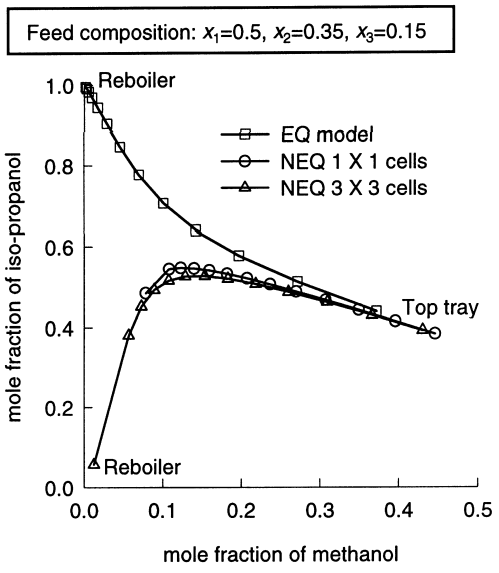

Fig. 6. Steady-state column composition trajectories for distillation of methanol (1) –*iso*-propanol (2) –water (3). Comparison of the response of EQ, NEQ 1×1 and NEQ 3×3 models.

Table 3
NRTL parameters for the mixtures methanol–*iso*-propanol–water

Component *i*	Component *j*	$A_{i,j}$ (J/mol)	$A_{j,i}$ (J/mol)	$\alpha_{i,j}$
Methanol	*iso*-Propanol	546.323	− 746.121	0.3040
Methanol	Water	− 1518.18	4943.753	0.2970
iso-Propanol	Methanol	587.483	6062.742	0.2880

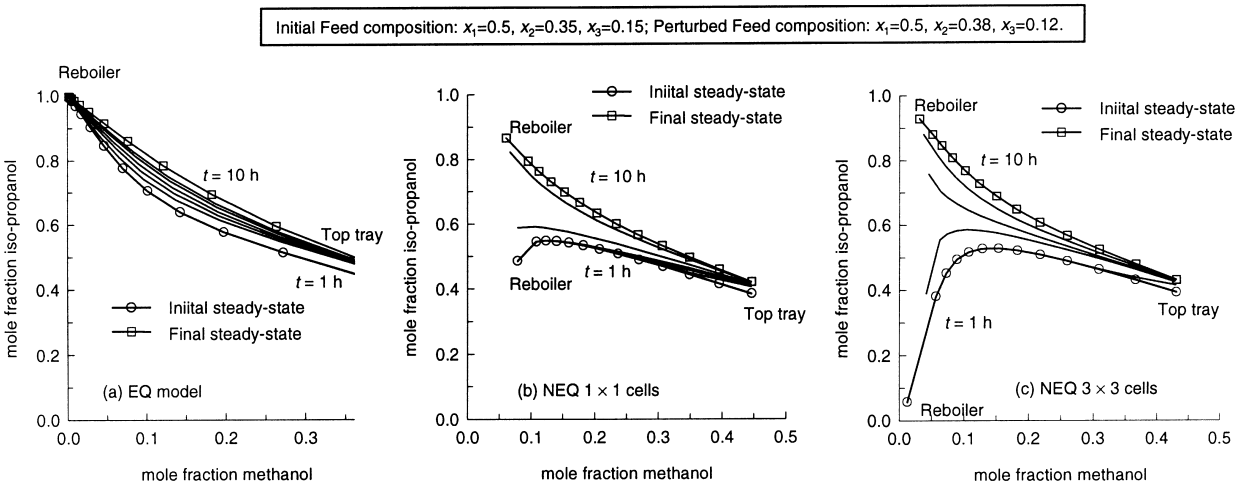

Fig. 7. Response to step disturbance in feed composition for distillation of methanol (1) –*iso*-propanol (2) –water (3). Comparison of the responses of EQ, NEQ 1 × 1 and NEQ 3 × 3 models.

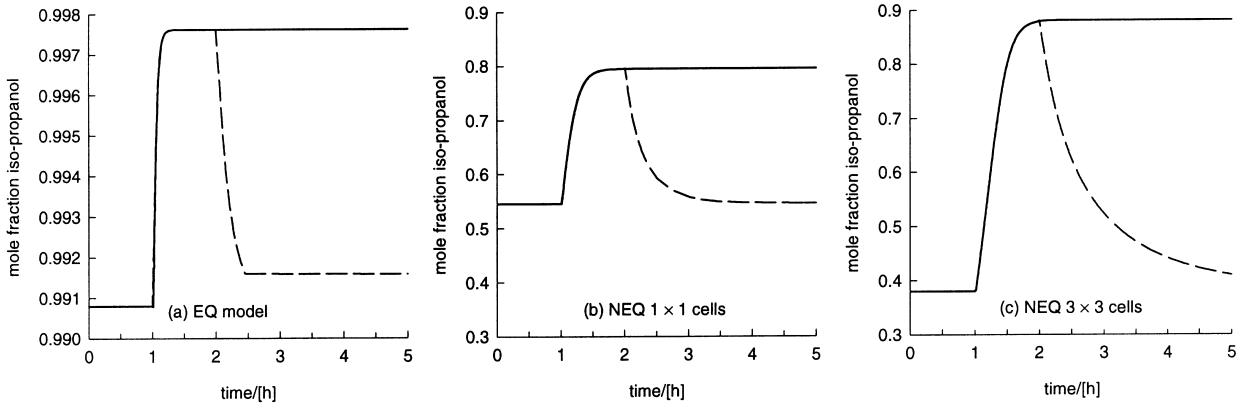

Fig. 8. Tray-12 composition response to pulse and step disturbance in feed composition for distillation of methanol (1) –*iso*-propanol (2) –water (3). Comparison of the responses of EQ, NEQ 1 × 1 and NEQ 3 × 3 models.

of overshoot and takes the longest time to recover to the initial steady state.

The need for using proper control strategies (and proper models!) is underlined when operating close to the distillation boundary.

5. Case study 3: dynamics of reactive distillation column for MTBE synthesis

Consider the synthesis of MTBE in an RD column. The column configuration chosen for the simulations is shown in Fig. 9; this is essentially the configuration described by Jacobs and Krishna (1993) in their simulation study using the EQ stage model. The total number of stages is 17, including a total condenser and a partial reboiler; the column pressure is 1115 kPa. Reactive stages are located in the middle of the column, stage 4 down to and including stage 11. The column has two feed streams: a methanol feed and a mixed butenes feed. A small stoichiometric excess of methanol is used. The mixed butenes feed, to stage 11, contains a mixture of *iso*-butene, which is reactive, and *n*-butene, which is nonreactive or inert. The reflux-ratio is set to 7 and the bottom flow rate is either set to 211 mol/s or varied (as a continuation parameter). The product removed from the top of the column is predominantly the inert *n*-butene. The bottoms product consists predominantly of MTBE. For a properly designed and operated column it is possible to achieve close to 100% conversion of *iso*-butene. The tray hardware details are specified in Table 2. The 5-liquid-pass tray configuration is shown in Fig. 10(a). On each of the eight stages in the reactive zone, 1000 kg of catalyst is introduced in the form of "envelopes" placed along the flow path length; see Fig. 10(b) and (c). The details of such a construction are available in

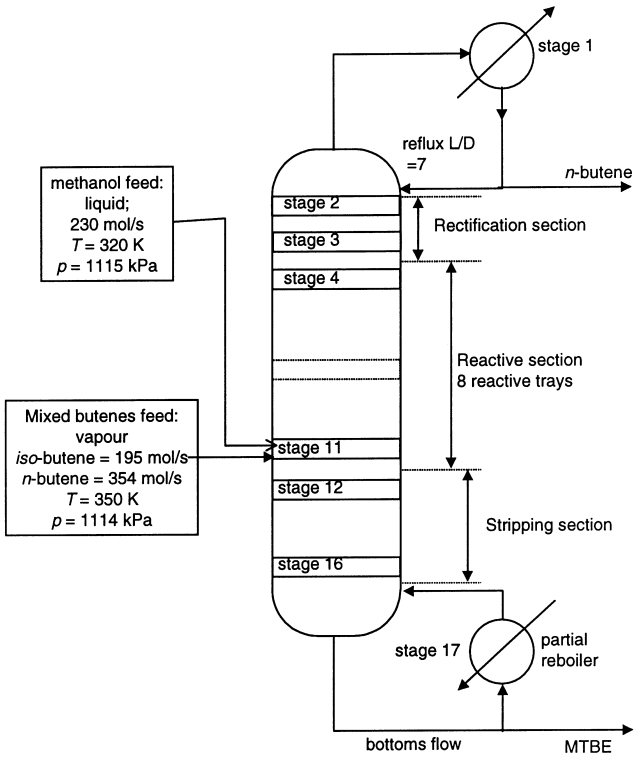

Fig. 9. Configuration of the MTBE synthesis column, following Jacobs and Krishna (1993). The column consists of 17 stages. The reactive stages are configured as sieve trays (see Fig. 10).

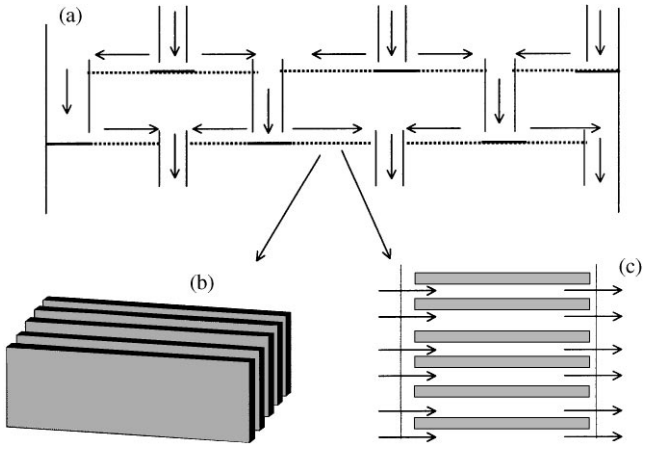

Fig. 10. (a) Five-liquid-pass sieve tray configuration. (b) and (c). The reactive section consists of catalyst envelopes placed along the liquid flow path.

the patent literature (Jones, 1985). The total amount of catalyst in the reactive zone is 8000 kg. The ion exchange capacity of the catalyst is 4.54 meq H^+/g.

The UNIQUAC model was used for description of liquid-phase nonideality, while the Soave–Redlich–Kwong equation of state was used for the vapour phase. The extended Antoine equation was used for calculation of the vapour pressure. Thermodynamic and kinetic data are taken from Rehfinger and Hoffmann (1990a,b).

The first objective of our dynamic simulations is to compare the results of EQ and NEQ multiple cell model. The separation capability of the nonreactive stripping and rectifying sections will also affect the overall column performance. We decided to focus on the differences of the EQ and NEQ modelling of the reactive section only and, therefore, assumed the nonreactive stages to have equal separation capability in both implementations. Towards this end, in the EQ model implementation we have assumed a tray efficiency of 65% for the nonreactive rectifying stages and 58% for the nonreactive stripping stages; these values corresponded closely to the calculations of the NEQ model for the corresponding nonreactive rectifying and stripping sections using the *A.I.Ch.E.* calculation method for sieve tray mass transfer. The interfacial area is estimated from the Hofhuis and Zuiderweg (1979) correlation and the fractional liquid hold-up on the tray is estimated from the correlation of Barker and Self (1962). Of course, in the NEQ model implementation of the nonreactive stages, efficiencies are not used in the calculations but can be calculated from the simulation results; these stage efficiencies vary for individual components. For the reactive section, the EQ model assumes vapour and liquid phases to be in thermodynamic equilibrium (however, not in reaction equilibrium).

Before performing dynamic simulations we used the continuation method to investigate the steady-state behaviour using the molar bottoms flow rate as the continuation parameter. The bifurcation diagrams for the NEQ model with 1×1, 2×2 and 3×3 cells are shown in Fig. 11. All three configurations show steady-state multiplicity. Clearly it is desirable to operate on the high-conversion branch of these curves; as is to be expected the conversion level on this branch increases with increasing degree of staging in the vapour and liquid phases. In fact, the bifurcation diagram for the NEQ 3×3 cell model coincides closely with that obtained by an EQ model; see Fig. 12.

The implication of the results in Fig. 12 is that when there is sufficient degree of staging in the liquid and vapour phases (3 well-mixed cells in either phases), the steady-state column performance corresponds to that of a column operating at thermodynamic equilibrium with the reaction rates determined by chemical kinetics. While the EQ model may be sufficient to describe the *steady-state* column performance under kinetically controlled conditions, we show below that the column *dynamics* could be significantly different when calculated with an NEQ model.

Taking the bottoms flow rate to be 211 mol/s, we performed dynamic simulations, starting with the high-conversion steady-state situation, and introducing a $+3$, $+5$ and $+7$% perturbation in the feed MeOH, 1 h after start-up. Fig. 13 shows the dynamic responses of the

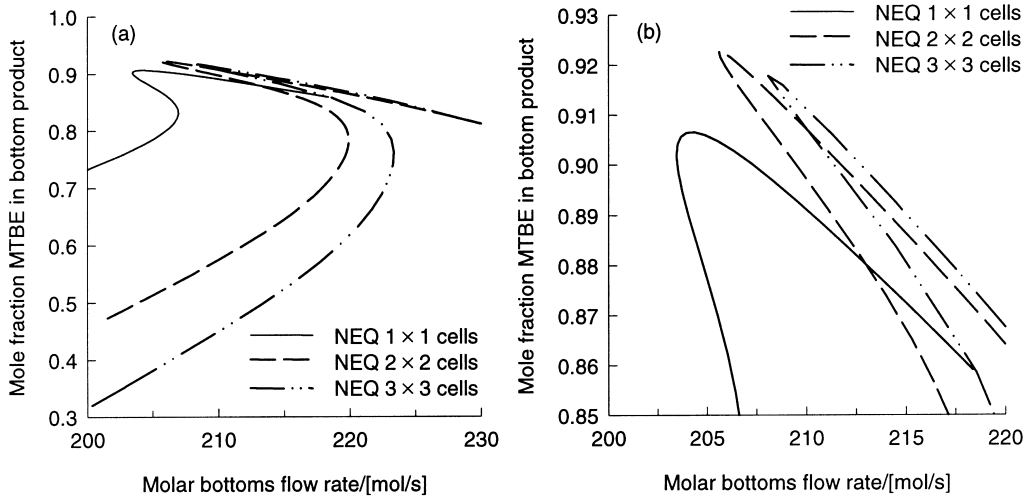

Fig. 11. Bifurcation diagram for three different model implementations, NEQ 1×1, NEQ 2×2 and NEQ 3×3 models. (a) and (b) represent the same information plotted on different scales.

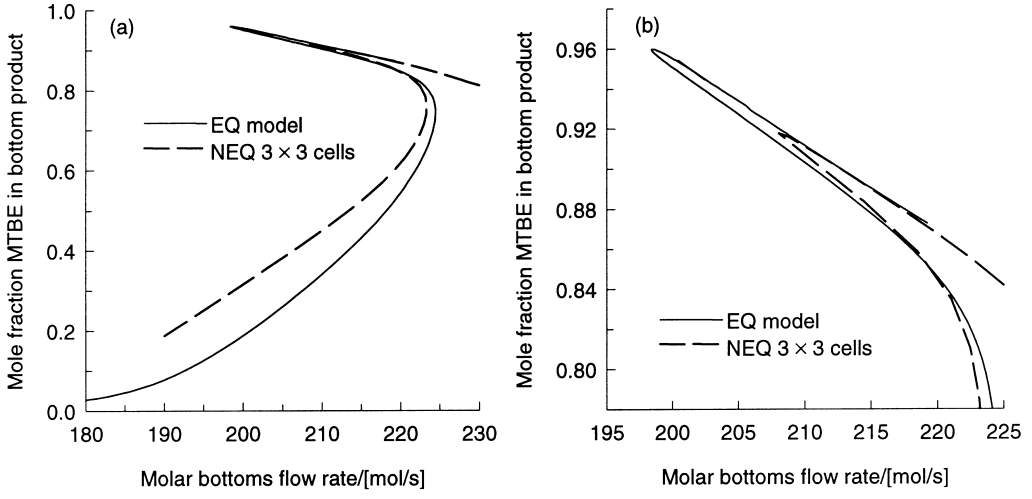

Fig. 12. Comparison of the bifurcation diagram for NEQ 3×3 cell model with EQ model. (a) and (b) represent the same information plotted on different scales.

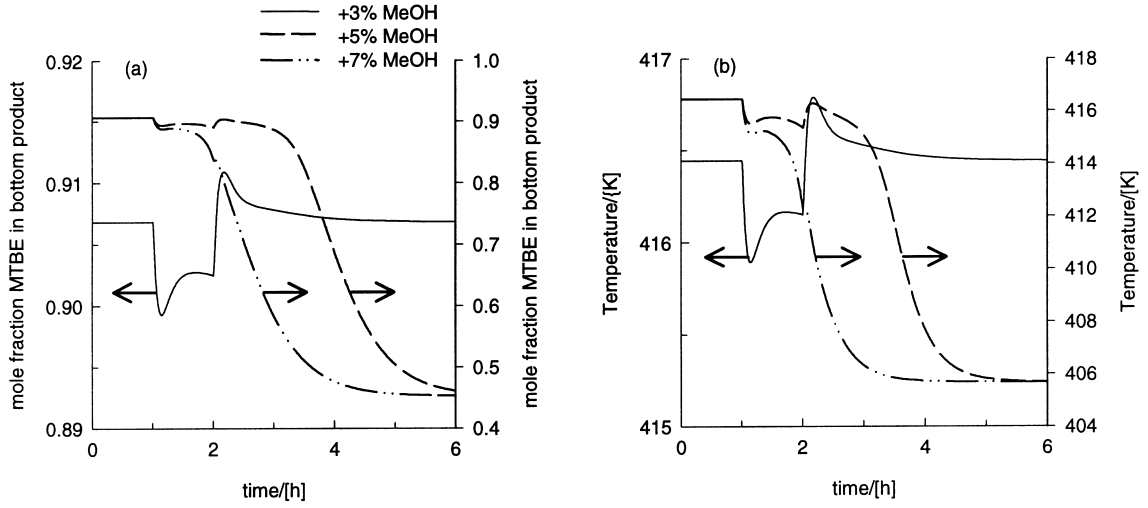

Fig. 13. Dynamic response obtained with the NEQ 3×3 cell model for MeOH feed flow perturbations (+ 3, + 5 and + 7%), 1 h after column start-up. The perturbation period is 1 h. (a) Response of MTBE bottom product composition and (b) response of bottom product temperature.

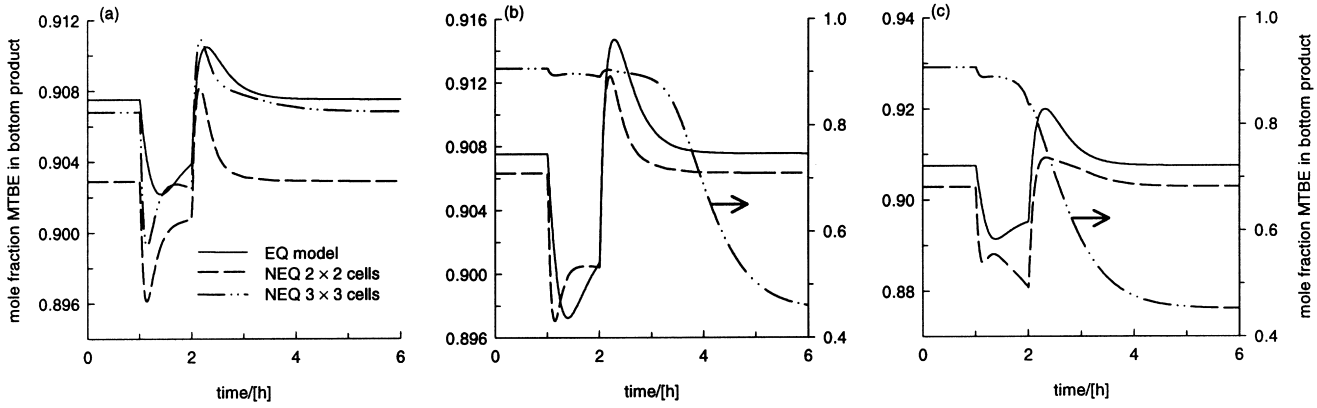

Fig. 14. Dynamic response obtained with the EQ, NEQ 2×2 and NEQ 3×3 models to MeOH feed flow perturbations of (a) $+3\%$, (b) $+5\%$ and (c) $+7\%$, 1 h after column start-up. The perturbation period is 1 h.

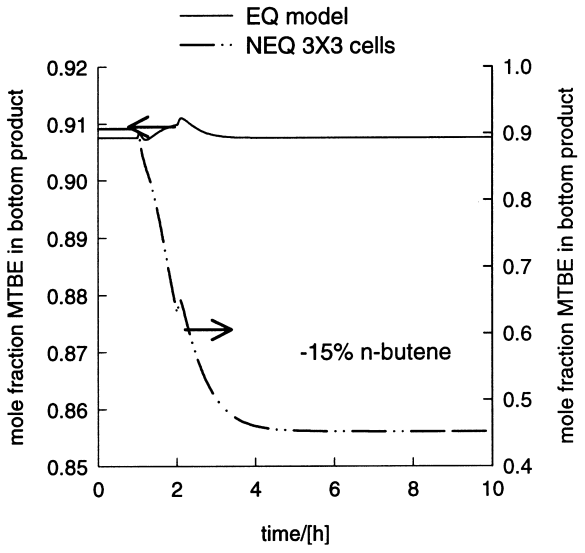

Fig. 15. Dynamic response obtained with the EQ and NEQ 3×3 models to a -15% feed flow perturbations of *n*-butene, 1 h after column start-up. The perturbation period is 1 h.

NEQ 3×3 model for the MTBE bottom production composition and temperature. It is interesting to note that for the $+5$ and $+7\%$ perturbations in the feed MeOH, the system suffers an (undesirable) transition from the high steady state to the lower one. Fig. 14 compares the response of the NEQ 2×2 and NEQ 3×3 models with the EQ model for (a) $+3\%$, (b) $+5\%$ and (c) $+7\%$ perturbation in the feed MeOH. From Fig. 14(a) we see that the responses of the EQ and NEQ 3×3 models are close to each other. However, when the magnitude of the perturbation is increased we see in Figs. 14(b) and (c) that the EQ and NEQ 3×3 models behave differently, both *quantitatively* and *qualitatively*. The NEQ 3×3 cell model suffers steady-state transitions whereas the EQ model recovers its initial high steady-state conversion.

For a -15% perturbation in the inert *n*-butene feed to the column, the dynamic responses are shown in Fig. 15. The EQ model is practically oblivious to this perturbation in the inert feed, whereas the NEQ 3×3 suffers transition from the high-conversion steady-state to the lower one.

6. Concluding remarks

We have developed a rigorous dynamic NEQ cell model for RD columns. The cell model becomes necessary in order to take account of staging of the vapour and liquid phases on a tray of an RD column.

The three case studies presented above lead to the following conclusions.

1. The introduction of staging in the liquid and vapour phases not only influences the steady-state performance, by increasing reaction conversion and separation capability, but also has an influence on column dynamics.
2. With the NEQ multiple-cells-per-stage model the column dynamics becomes more sensitive to perturbations when compared to the EQ stage model.
3. When operating close to the distillation boundary for nonreactive, conventional, distillation, the use of the rigorous Maxwell–Stefan diffusion equations to describe mass transfer can result in completely different composition trajectories from that predicted by an EQ model *even for steady-state operation*. Even small feed composition perturbations could lead to completely different compositions of products.
4. Even when the NEQ multiple-cell and EQ stage models exhibit almost identical *steady-state* characteristics, the *dynamic* responses of an RD column to perturbations could be significantly different.

The results presented in Figs. 12–15 provide convincing evidence to support the contention of Doherty and

Buzad (1992) who wrote "...steady state simulations are inadequate for assessing the effectiveness of operability and control schemes for reactive distillation columns... control schemes with good steady-state measures frequently fail under dynamic conditions, and that the failure was discovered only by using the full nonlinear dynamic simulation. ....There are good opportunities for productive research in this area, including such effects as the existence of multiple steady-states in reactive distillation and strategies for operating at the desired one".

We add one rider to the remark of Doherty and Buzad (1992) that nonequilibrium dynamic models, such as those described in this paper, taking proper account of interphase mass transfer and of liquid and vapour staging on a tray, are essential for developing the proper control strategies for RD columns.

Notation

a	interfacial area per unit volume, m^{-1}
A	interfacial area, m^2
A_{bub}	active (bubbling) area on tray, m^2
c	number of components in the mixture
c_t	total concentration, mol/m^3
$Đ_{i,k}$	Maxwell–Stefan diffusivity, m^2/s
E	energy holdup, J
$\mathbb{E}$	energy transfer rate, J/s
F	feed stream, mol/s
h_{cl}	clear liquid height, m
h_t	tray spacing, m
h_w	weir height, m
H	molar enthalpy, J/mol
h	heat transfer coefficient, W/m^2 K
K	vapour-liquid equilibrium constant
K_{eq}	metathesis reaction equilibrium constant
L	liquid flow rate, mol/s
L_M	liquid interchange mixing flow rate, mol/s
m	number of cells along the liquid flow direction
M_i	molar hold-up of component i, mol
n	number of cells along the vapour flow direction
nL	number of grid cells in liquid diffusion film
nV	number of grid cells in vapour diffusion film
$\mathbb{N}$	mass transfer rate, mol/s
Q	heat duty, J/s
r	number of reactions
$R_{i,j}$	reaction rate, mol/m^3 s
$\mathbb{R}$	gas constant, J/mol K
T	temperature, K
V	vapour flow rate, mol/s
W	weir length, m
x	mole fraction in the liquid phase
y	mole fraction in the vapour phase
z	mole fraction in the feed stream

Greek letters

ε	volumetric hold-up of phase, m^3
δ	diffusion film thickness, m
η	dimensionless coordinate, dimensionless
κ	mass transfer coefficient, m/s
μ	chemical potential, J/mol

Subscripts

i	component index
in	stream entering cell
j	stage index
I	interface
k	index
$M+$	property of the cell above the one under consideration
$M-$	property of the cell above the one under consideration
mm	index for cells in a row
nn	index for cells in a column
t	total

Superscripts

F	feed stream
L	liquid phase
Lf	liquid diffusion film
V	vapour phase
Vf	vapour diffusion film

Acknowledgements

Partial support for our work comes from BP-Amoco Chemicals. RB and RK gratefully acknowledge financial support from the Netherlands Organisation for Scientific Research (NWO) in the form of a "programmasubsidie".

References

Abufares, A. A., & Douglas, P. L. (1995). Mathematical modeling and simulation of an MTBE catalytic distillation process using SPEEDUP and AspenPlus. *Chemical Engineering Research and Design, Transactions of the Institution of Chemical Engineers, Part A*, *73*, 3–12.

Alejski, K., & Duprat, F. (1996). Dynamic simulation of the multicomponent reactive distillation. *Chemical Engineering Science*, *51*, 4237–4252.

Barker, P. E., & Self, M. F. (1962). The evaluation of liquid mixing effects on a sieve plate using unsteady and steady state tracer techniques. *Chemical Engineering Science*, *17*, 541–554.

Bartlett, D. A., & Wahnschafft, O. M. (1998). Dynamic simulation and control strategy evaluation for MTBE reactive distillation. In J. F. Pekny, & G. E. Blau (Eds.), *Foundations of computer-aided process operation*, A.I.Ch.E. Symposium Series, vol. 320 (pp. 315–321).

Baur, R., Higler, A. P., Taylor, R., & Krishna, R. (2000). Comparison of equilibrium stage and nonequilibrium stage models for reactive distillation. *Chemical Engineering Journal*, *76*, 33–47.

Baur, R., Taylor, R., Krishna, R., & Copati, J. A. (1999). Influence of mass transfer in distillation of mixtures with a distillation boundary. *Chemical Engineering Research and Design, Transactions of the Institution of Chemical Engineers, Part A*, *77*, 561–565.

Bennett, D. L., Agrawal, R., & Cook, P. J. (1983). New pressure drop correlation for sieve tray distillation columns. *American Institute of Chemical Engineers Journal*, *29*, 434–442.

Bennett, D. L., & Grimm, H. J. (1991). Eddy diffusivity for distillation sieve trays. *American Institute of Chemical Engineers Journal*, *37*, 589–596.

Bulirsch, R., & Stoer, J. (1966). Numerical treatment of ordinary differential equations by extrapolation methods. *Numerical Mathematics*, *8*, 1–13.

Ciric, A. R., & Miao, P. (1994). Steady state multiplicities in an ethylene glycol reactive distillation column. *Industrial and Engineering Chemistry Research*, *33*, 2738–2748.

Doherty, M. F., & Buzad, G. (1992). Reactive distillation by design. *Chemical Engineering Research and Design, Transactions of the Institution of Chemical Engineers, Part A*, *70*, 448–458.

Espinosa, J., Martinez, E., & Perez, G. A. (1994). Dynamic behavior of reactive distillation columns, Equilibrium systems. *Chemical Engineering Communications*, *128*, 19–42.

Grosser, J. H., Doherty, M. F., & Malone, M. F. (1987). Modeling of reactive distillation systems. *Industrial and Engineering Chemistry Research*, *26*, 983–989.

Güttinger, T. E., & Morari, M. (1999a). Predicting multiple steady states in equilibrium reactive distillation. 1. Analysis of nonhybrid systems. *Industrial and Engineering Chemistry Research*, *38*, 1633–1648.

Güttinger, T. E., & Morari, M. (1999b). Predicting multiple steady states in equilibrium reactive distillation. 2. Analysis of hybrid systems. *Industrial and Engineering Chemistry Research*, *38*, 1649–1665.

Hauan, S., Hertzberg, T., & Lien, K. M. (1995). Why methyl- *tert*-butyl-ether production by reactive distillation may yield multiple solutions. *Industrial and Engineering Chemistry Research*, *34*, 987–991.

Higler, A., Krishna, R., & Taylor, R. (1999a). A nonequilibrium cell model for multicomponent (reactive) separation processes. *American Institute of Chemical Engineers Journal*, *45*, 2357–2370.

Higler, A., Krishna, R., & Taylor, R. (1999b). A non-equilibrium cell model for packed distillation columns. The influence of maldistribution. *Industrial and Engineering Chemistry Research*, *38*, 3988–3999.

Higler, A., Krishna, R., & Taylor, R. (2000). Non-equilibrium modelling of reactive distillation: A dusty fluid model for heterogeneously catalysed processes. *Industrial and Engineering Chemistry Research*, *39*, 1596–1607.

Higler, A. P., Taylor, R., & Krishna, R. (1998). Modeling of a reactive separation process using a nonequilibrium stage model. *Computers and Chemical Engineering*, *22*, S111–S118.

Higler, A. P., Taylor, R., & Krishna, R. (1999c). Nonequilibrium modelling of reactive distillation: Multiple steady states in MTBE synthesis. *Chemical Engineering Science*, *54*, 1389–1395.

Higler, A. P., Taylor, R., & Krishna, R. (1999d). The influence of mass transfer and liquid mixing on the performance of reactive distillation tray column. *Chemical Engineering Science*, *54*, 2873–2881.

Hofhuis, P. A. M., & Zuiderweg, F. J. (1979). Sieve plates: Dispersion density and flow regimes. *Institution of Chemical Engineers Symposium Series No. 56* (pp. 2.2/1–2.2/26).

Jacobs, R., & Krishna, R. (1993). Multiple Solutions in reactive distillation for methyl-*tert*-butyl ether synthesis. *Industrial and Engineering Chemistry Research*, *32*, 1706–1709.

Jones Jr., E. M. (1985). Contact structure for use in catalytic distillation, U.S. Patent 4536373.

Kooijman, H. A. (1995). *Dynamic nonequilibrium column simulation.* Ph.D. dissertation, Clarkson University: Potsdam, USA.

Kooijman, H. A., & Taylor, R. (1995). A dynamic nonequilibrium model of tray distillation columns. *American Institute of Chemical Engineers Journal*, *41*, 1852–1863.

Kreul, L. U., Gorak, A., Dittrich, C., & Barton, P. I. (1998). Dynamic catalytic distillation: Advanced simulation and experimental validation. *Computers and Chemical Engineering*, *22*, S371–S378.

Krishna, R., & Wesselingh, J. A. (1997). The Maxwell–Stefan approach to mass transfer. *Chemical Engineering Science*, *52*, 861–911.

Kröner, A., Marquardt, W., & Gilles, E. D. (1997). Getting around consistent initialization of DAE systems?. *Computers and Chemical Engineering*, *21*, 145–158.

Kubicek, M. (1976). Algorithm 502, dependence of a solution of nonlinear systems on a parameter. *ACM Transactions on Mathematical Software*, *2*, 98–107.

Kumar, A., & Daoutidis, P. (1999). Modeling, analysis and control of ethylene glycol reactive distillation column. *American Institute of Chemical Engineers Journal*, *45*, 51–68.

Lockett, M. J. (1986). *Distillation tray fundamentals*. Cambridge, UK: Cambridge University Press.

Mattsson, S. E., & Sönderlind, G. (1993). Index-reduction using dummy derivatives. *SIAM Journal on Scientific Statistical Computing*, *14*, 677–692.

Michelsen, M. (1976). An efficient general purpose method of integration of stiff ordinary differential equations. *American Institute of Chemical Engineers Journal*, *22*, 594–597.

Mohl, K. D., Kienle, A., Gilles, E. D., Rapmund, P., Sundmacher, K., & Hoffmann, U. (1999). Steady-state multiplicities in reactive distillation columns for the production of fuel ethers MTBE and TAME: Theoretical analysis and experimental verification. *Chemical Engineering Science*, *54*, 1029–1043.

Moe, H. I., Hauan, S., Lien, K. M., & Hertzberg, T. (1995). Dynamic model of a system with phase and reaction equilibrium. *Computers and Chemical Engineering*, *19*, S513–S518.

Muller, N. P., & Segura, H. (2000). An overall rate-based stage model for cross-flow distillation columns. *Chemical Engineering Science*, *55*, 2515–2528.

Nijhuis, S. A., Kerkhof, F. P. J. M., & Mak, A. N. S. (1993). Multiple steady states during reactive distillation of methyl-*tert*-butyl-ether. *Industrial and Engineering Chemistry Research*, *32*, 2767–2774.

Okasinski, M. J., & Doherty, M. F. (1998). Design method for kinetically controlled, staged reactive distillation columns. *Industrial and Engineering Chemistry Research*, *37*, 2821–2834.

Pelkonen, S., Kaesemann, R., & Gorak, A. (1997). Distillation lines for multicomponent separation in packed columns: Theory and comparison with experiments. *Industrial and Engineering Chemistry Research*, *36*, 5302–5398.

Perez-Cisneros, E., Schenk, M., Gani, R., & Pilavachi, P. A. (1996). Aspects of simulation, design and analysis of reactive distillation operations. *Computers and Chemical Engineering*, *20*, S267–S272.

Rapmund, P., Sundmacher, K., & Hoffmann, U. (1998). Multiple steady states in a reactive distillation column for the production of the fuel ether TAME II. Experimental Validation. *Chemical Engineering and Technology*, *21*, 136–139.

Rehfinger, A., & Hoffmann, U. (1990a). Kinetics of methyl-*tert*-butyl ether liquid phase synthesis catalyzed by ion exchange resin. I — intrinsic rate expression in liquid phase activities. *Chemical Engineering Science*, *45*, 1605–1616.

Rehfinger, A., & Hoffmann, U. (1990b). Kinetics of methyl-*tert*-butyl ether liquid phase synthesis catalyzed by ion exchange resin, II — macropore diffusion of MeOH as rate controlling step. *Chemical Engineering Science*, *45*, 1619–1626.

Roat, S. D., Downs, J. J., Vogel, E. F., & Doss, J. E. (1986). The integration of rigorous dynamic modeling and control system

synthesis for distillation columns: An industrial approach. In: M. Morari, & T. J. McAvoy (Eds.), *Chemical Process Control — CPC III*. New York: Elsevier.

Ruiz, C. A., Basualdo, M. S., & Scenna, N. J. (1995). Reactive distillation dynamic simulation. *Chemical Engineering Research and Design, Transactions of the Institution of Chemical Engineers, Part A*, *73*, 363–378.

Scenna, N. J., Ruiz, C. A., & Benz, S. J. (1998). Dynamic simulation of startup procedures of reactive distillation columns. *Computers and Chemical Engineering*, *22*, S719–S722.

Schrans, S., de Wolf, S., & Baur, R. (1996). Dynamic simulation of reactive distillation, An MTBE case study. *Computers and Chemical Engineering*, *20*(Suppl.), S1619–S1624.

Seader, J. D., & Henley, E. J. (1998). *Separation process principles*. New York: Wiley.

Sneesby, M. G., Tadé, M. O., & Smith, T. N. (1998). Steady-state transitions in the reactive distillation of MTBE. *Computers and Chemical Engineering*, *22*, 879–892.

Sundmacher, K., Uhde, G., & Hoffmann, U. (1999). Multiple reactions in catalytic distillation processes for the production of the fuel oxygenates MTBE and TAME: Analysis by rigorous model and experimental validation. *Chemical Engineering Science*, *54*, 2839–2847.

Taylor, R., Kooijman, H. A., & Hung, J. S. (1994). A second generation nonequilibrium model for computer simulation of multicomponent separation processes. *Computers and Chemical Engineering*, *18*, 205–217.

Taylor, R., & Krishna, R. (1993). *Multicomponent mass transfer*. New York: Wiley.

Taylor, R., & Krishna, R. (2000). Modelling reactive distillation. *Chemical Engineering Science*, *55*, 5188–5228.

Unger, J., Kröner, A., & Marquardt, W. (1995). Structural analysis of differential-algebraic equation systems — theory and applications. *Computers and Chemical Engineering*, *19*, 867–882.

Wayburn, T. L., & Seader, J. D. (1987). Homotopy continuation methods for computer aided process design. *Computers and Chemical Engineering*, *11*, 7–25.